



Impact of pump-signal overlap in S+C+L band discrete Raman amplifiers

MD ASIF IQBAL,^{1,*}  GABRIELE DI ROSA,^{2,3}  LUKASZ KRZCZANOWICZ,¹ IAN PHILLIPS,¹ PAUL HARPER,¹ ANDRÉ RICHTER,² AND WLADEK FORYSIAK¹ 

¹Aston Institute of Photonics Technologies, Aston University, Birmingham B4 7ET, UK

²VPIphotonics GmbH, Carnotstr. 6, Berlin, Germany

³Technische Universität Berlin, Straße des 17. Juni 135, Berlin, Germany

*a.iqbal25@aston.ac.uk

Abstract: We experimentally investigate the impact of pump-signal overlap in ultra-wideband (>13THz) Raman amplifiers and measure the transmission penalty on 30GBaud PM-QPSK signals due to adjacent Raman pumps in a 15dB gain, 150nm (~18.8THz) S+C+L-band discrete Raman amplifier. We present an efficient numerical model to predict the performance penalty induced by crosstalk from Rayleigh backscattered light from backward-propagating Raman pumps showing good agreement with the experimental results. A 4nm guard-band must be retained around an overlapping Raman pump based on typical, commercial semiconductor laser pump diodes to ensure a negligible transmission penalty in S-band.

Published by The Optical Society under the terms of the [Creative Commons Attribution 4.0 License](https://creativecommons.org/licenses/by/4.0/). Further distribution of this work must maintain attribution to the author(s) and the published article's title, journal citation, and DOI.

1. Introduction

It is important to optimise the design of ultra-wideband (UWB) optical amplifiers to increase the total capacity of currently deployed standard single mode fibre (SSMF) based optical transmission systems by nearly 10-fold compared with the presently exploited erbium doped fibre amplifier (EDFA) C-band. Recently, multi-band transmission strategies using rare-earth doped fibre amplifiers in different bands have been proposed to increase the system capacity of existing optical fibre networks [1,2]. UWB transmission experiments over S+C+L band have already been reported using different rare-earth doped fibre amplifiers operating over separate discrete bands as well as continuous single band semiconductor optical amplifiers (SOAs) [3,4]. Discrete Raman amplifiers (DRAs) also offer continuous, flat and UWB amplification using stimulated Raman scattering (SRS) from a set of multiplexed Raman pumps through a suitable gain fibre [5–7]. However, when the amplification bandwidth exceeds the Raman Stokes shift of ~13THz, Raman pumps co-exist with signals in parts of the spectrum resulting in additional penalties to the adjacent signals, due to fundamental Rayleigh backscattering (RBS) pump light induced crosstalk and Kerr nonlinearities from relatively high power pump components [8,9]. Additionally, the use of small core area fibre with high nonlinear coefficient in high gain UWB DRAs may cause strong pump broadening and generation of high nonlinear Kerr product power components, which can degrade the optical signal to noise ratio (OSNR) of the neighbouring signals and reduce the effective transmission capacity of the system [9]. The use of narrowing and rejection filters has been proposed to reduce the impact of crosstalk from overlapping pumps in UWB distributed Raman amplifiers [10,11]. However, these additional passive components introduce undesirable extra losses.

In our previous study [12], we experimentally demonstrated an improved design of UWB DRA with high gain and low overall noise figure by using a dual-stage configuration with an appropriate distribution of Raman pumps. We also experimentally quantified the transmission

penalties induced by crosstalk from overlapping Raman pumps in a high gain (~ 15 dB) S+C+L band dual-stage DRA [13]. Here, we experimentally and numerically demonstrate that the OSNR degradation and corresponding transmission penalties from overlapping commercial semiconductor Raman pump laser diodes depend on both the RBS level and spectral linewidth of the Raman pump lasers. Our proposed numerical model is low complexity and shows very good agreement with the experimentally measured transmission penalty induced by RBS generated by backward propagating Raman pumps in an UWB DRA. We report that a negligible Q^2 -penalty on the neighbouring 30GBaud PM-QPSK signals can be achieved by retaining a guard-band of ~ 4 nm around the Raman pump. Additionally, >4 dB Q^2 -penalty is observed on signals within 1.5nm of the pump having a RBS level up to the amplified signal.

2. Experimental setup

The UWB transmission experiment setup used a 70km SSMF and a 150nm bandwidth S+C+L-band (1475-1625nm) DRA as shown in Fig. 1.

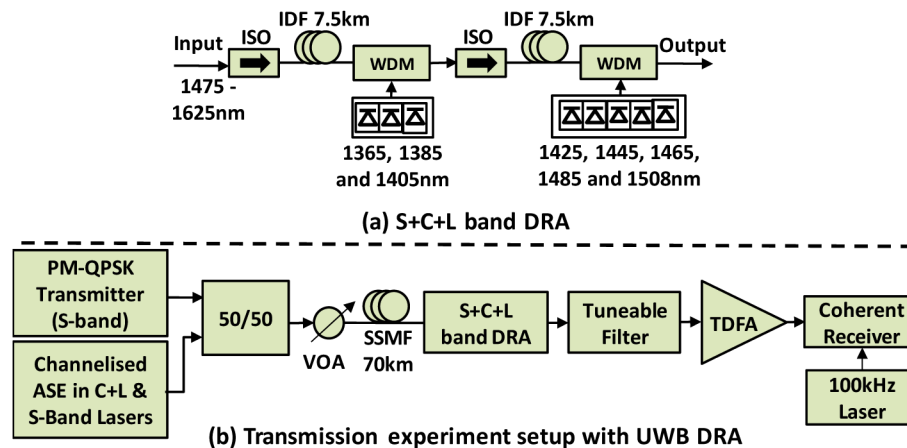


Fig. 1. (a) Schematic of the S+C+L band DRA; (b) Transmission experiment setup.

The ~ 15 dB transmission loss from the 70km SSMF was compensated by a dual-stage UWB DRA which improves the overall net gain and noise figure by properly distributing the Raman pumps in two stages [12]. A 7.5km long inverse dispersion fibre (IDF) was chosen as the Raman gain fibre in each stage and backward-pumping was used to avoid pump to signal relative intensity noise transfer [14,15]. The first stage was pumped with three Raman pumps (1365, 1385 and 1405nm) which mainly provided gain in the S-band. In the second stage, five pumps (1425, 1445, 1465, 1485 and 1508nm) were used to provide gain mainly in the C+L band. This dual-stage architecture reduces the strong pump depletion of shorter wavelength pumps by inhibiting the pump-to-pump Raman energy transfer and so enables an overall flat net gain of ~ 15 dB at the output. However, the 1485nm and 1508nm pumps, which are required to provide gain for L-band signals, fall directly in the S-band and RBS arising from these pumps co-propagate with S-band signals through the second stage of the DRA introducing crosstalk penalty on neighbouring channels.

In the experiment, eight available pump wavelengths were chosen at every ~ 20 nm from 1365 nm to 1508 nm to ensure flat gain spectrum across 150 nm bandwidth. The net gain was calculated comparing the input and output spectra of the DRA and the pump powers were optimised carefully to obtain overall net gain variation < 3 dB across the 150 nm amplification bandwidth. At first, the proposed dual-stage DRA was numerically simulated and then, required

pump powers to maintain < 3 dB gain variation was obtained using the Raman optimiser tool of VPIphotonics Design Suite 10.0 which uses a genetic algorithm for pump power optimisation [16]. However, further improvement of gain variation may be achieved by optimising both the pump wavelengths and powers through a hybrid genetic algorithm [17], or via inverse system design using machine learning [18]. The pump powers used in the experiment are given in Table 1.

Table 1. Pump powers used in the UWB dual-stage DRA

Stage	First stage				Second stage			
Pump wavelength (nm)	1365	1385	1405	1425	1445	1465	1485	1508
Pump power (mW)	305	490	180	370	330	188	87	186

At the receiver, the PM-QPSK signal was filtered out using a tuneable bandpass filter and amplified using a commercial thulium doped fibre amplifier (TDFA) before passing onto the coherent receiver where the signals were received with an 80GSa/s, 36GHz bandwidth oscilloscope and digitally processed offline.

The input to the 70 km SSMF span and output from the dual-stage DRA is shown in Fig. 2(a). The input WDM signal consisted of: (i) a tuneable 30GBaud PM-QPSK signal and three CW lasers in S-band at 1475 nm, 1490 nm and 1500 nm (ii) 24 shaped ASE channels from C- and L-band EDFAs in C+L band (1530-1605 nm), and (iii) a fixed CW laser at the longest wavelength of 1625 nm, included to confirm the full extent of the L-band DRA gain. The channelised ASE noise from C and L band EDFAs was spectrally shaped with 50 GHz 3 dB bandwidth and 300 GHz channel spacing using wavelength selective switches. The total WDM signal power at the input of the span was 15dBm with a flat spectrum except the three S-band CW DFB lasers which were limited in maximum output power. In Fig. 2(a), the RBS light of the 1508nm pump was much higher than that of the 1485nm pump because of its higher power and greater pump-to-pump energy transfer from the lower wavelength pumps. Consequently, the crosstalk penalties due to the 1508nm pump are expected to be higher than those due to its 1485nm counterpart. At the receiver, the impact on the transmission performance of the PM-QPSK signal was measured by sweeping the carrier wavelength around the overlapping pumps' central wavelength.

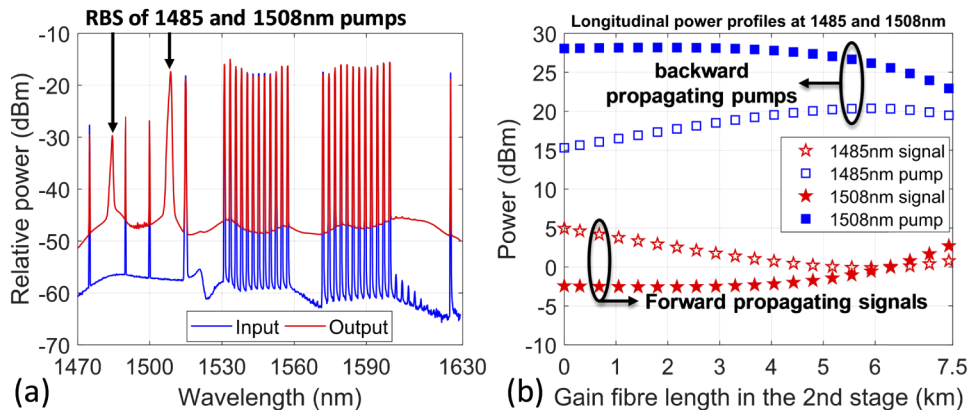


Fig. 2. (a) Measured input to the SSMF span and output spectra from the UWB DRA; (b) Numerically simulated power profiles of signals and pumps at 1485 nm and 1508 nm along the 7.5 km IDF second stage.

3. Numerical model and simulation setup

In the numerical simulation, a similar transmission setup with the dual-stage UWB DRA has been considered as in Fig. 1. Two 30GBaud QPSK modulated signals shaped using a raised cosine filter with 0.2 roll-off factor were used in the S-band around the overlapping 1485nm and 1508nm pumps. The central wavelength of the modulated signals were swept across the overlapping pumps' spectra in a range of ± 3.2 nm. In C- and L-bands, the WDM channels were represented by single spectral lines in order to consider the Raman energy transfer and overall gain efficiently. The wavelength dependent loss, Raman gain coefficient and other parameters of IDF and SSMF used in the numerical model are as previously described [19,20]. The Rayleigh backscattering coefficient of IDF was considered as $\gamma_r = 1.6 \times 10^{-7} \text{ m}^{-1}$. Additive white Gaussian noise (AWGN) was added to the signal at the input to maintain common reference back-to-back (B-2-B) Q^2 -factors as measured in the experiment at 1485 nm and 1508 nm, without considering RBS impact from the DRA.

In the derivation of the numerical model, we consider that the definition of the Q^2 -factor has an equivalent description of signal to noise ratio (SNR) in a noise limited system. Accordingly, we define $SNR_{ref}(\lambda)$ as the value that corresponds to the reference Q^2 -factor for $\lambda_i = \{1485, 1508\}$ nm when the impact of RBS induced penalty is negligible because a sufficiently large guard-band is maintained between the pump and signal wavelengths. The RBS induced penalty is included in the calculation of total SNR as:

$$SNR_{tot}(\lambda) = \frac{P_S^+(z=L, \lambda)}{\frac{P_S^+(z=L, \lambda)}{SNR_{ref}(\lambda_i)} + P_{RBS}^+(z=L, \lambda)} \quad (1)$$

Here, $P_S^+(z=L, \lambda)$ and $P_{RBS}^+(z=L, \lambda)$ are the signal and RBS forward propagating power at the output of the DRA. To estimate these two components, we calculate the longitudinal evolution of the signal P_S^+ and backward propagating pump P_P^- , via a system of coupled differential equations solved numerically along the length of the DRA $z \in [0, L]$ [5,21], using the model included in VPIphotonics Design Suite 10.0 as shown in Fig. 2(b). In these calculations, the broadband Raman pumps were considered as monochromatic spectral components at wavelengths λ_i , an approximation which provided reliable results while significantly decreasing the computational complexity of the Raman solver. Once P_S^+ and P_P^- have been obtained in the range $z \in [0, L]$, the problem reduces to the estimation of $P_{RBS}^+(z=L, \lambda)$. We also neglected the co-propagating multi-path interference of the signal, in view of the much higher power level of the overlapping pumps. Hence, $P_{RBS}^+(z=L, \lambda)$ has been estimated as the sum of all the RBS contributions from the pump which are generated along the DRA, appropriately scaled by the gain or attenuation they are subject to when propagating from the generation point to $z=L$. Spatially dividing the amplifier into infinitesimally small sections dz , we can then write:

$$P_{RBS}^+(z=L, \lambda) = \int_0^L \gamma_r P_P^-(\lambda, z) \frac{P_S^+(L, \lambda)}{P_S^+(z, \lambda)} dz \quad (2)$$

where P_P^- is the pump power that falls inside the receiver bandwidth propagating over the length of the DRA. This term takes into account the spectral shape of the broadband pump, which proved to be a key consideration to obtain reliable predictions.

4. Results and discussion

The penalties due to the crosstalk and Kerr induced nonlinear products arising from the relatively high power backward propagating 1485nm and 1508nm Raman pumps depend mainly on the launched power of these pumps and their spectral properties.

The spectral profiles of the two overlapping commercial semiconductor laser diode pumps at 1485nm and 1508nm with 3dB linewidth ~ 1 nm are shown in Fig. 3(a) and Fig. 3(b), respectively. The typical linewidth of semiconductor pump laser diodes is usually 1-1.5nm, however side-lobes (residual ASE due to imperfect fibre Bragg grating properties) can spread out a few nanometers away from the central wavelength as shown in the spectrum of the 1508nm pump in Fig. 3(b). Moreover, the strength of these side-lobes can become significant under some operating conditions i.e. temperatures, drive currents, and need to be filtered out by proper design of Raman pump combiners or via narrowing filters [10]. In our experiment, the side-lobe of the 1508nm pump had very low power compared with the main peak, so the RBS components from this side-lobe introduced negligible crosstalk penalty on the WDM signals, compared with the main-lobe.

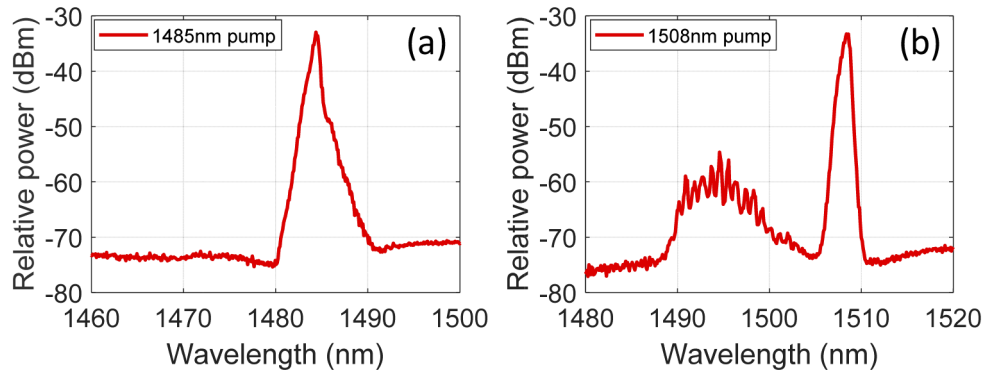


Fig. 3. Spectra of the overlapping (a) 1485 nm and (b) 1508 nm pumps.

The spectra of the received and bandpass filtered PM-QPSK signals adjacent to the two overlapping pumps are shown in Fig. 4(a) and Fig. 4(b), respectively. It can be clearly seen that the received signal OSNR degrades as it moves closer to the overlapping pump, and OSNR degradation of the signals near to the 1508nm pump is much higher than those near to the 1485nm pump, which is mainly due to the greater impact of crosstalk from the relatively higher 1508nm launch pump power leading to >13 dB RBS level in comparison, as shown in Fig. 2(a).

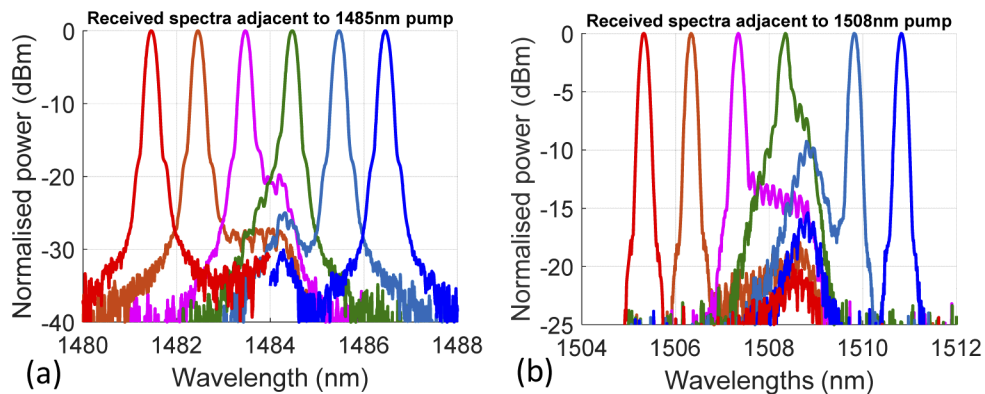


Fig. 4. Received spectra of PM-QPSK signals adjacent to (a) 1485 nm and (b) 1508 nm pump.

At the receiver, we measured the Q^2 -factors of the S-band signals adjacent to the overlapping pumps by varying the signal wavelengths until there was no significant transmission penalty from the pump induced crosstalk, as shown in Fig. 5.

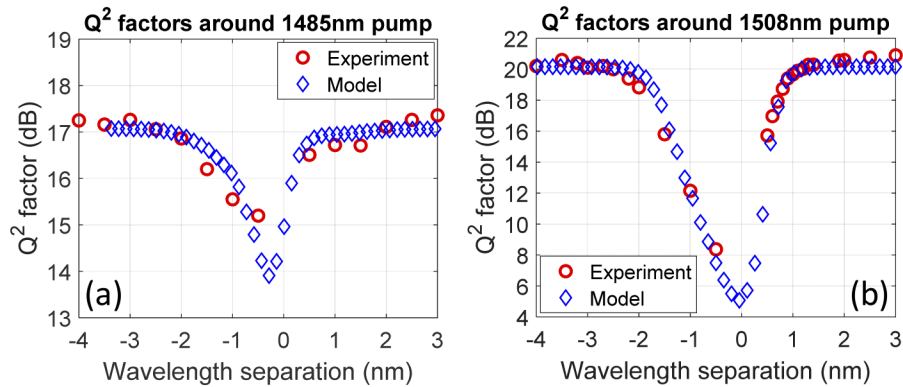


Fig. 5. Q^2 -factors vs wavelength separation with respect to (a) 1485 nm and (b) 1508 nm pump.

The average B-2-B Q^2 -factors for the PM-QPSK signals adjacent to the overlapping pumps in the 1482-1488nm and 1504-1511nm wavelength regions were 19.3dB and 21.3dB, respectively. After 70km SSMF transmission, the additional penalties from the B-2-B Q^2 -factors around the 1485nm pump (Fig. 5(a)) compared to the 1508nm (Fig. 5(b)) were higher due to the lower OSNR of the transmitted signals, lower available power of the local oscillator in the coherent receiver, and additional Kerr induced nonlinear penalties through the first stage of the DRA [12]. It is also clear from Fig. 5 that the Q^2 penalties to the signals adjacent to the higher power 1508nm pump are greater than those in the vicinity of the 1485nm pump, which is consistent with the higher level of RBS and greater OSNR penalties shown in Fig. 2(a) and Fig. 4, respectively. The exact wavelength of the 1485nm pump used in the experiment was measured to be ~ 1484.8 nm and the model accurately predicts the worst Q^2 penalty of ~ 3 dB at 0.2nm downshifted from 1485nm, as shown in Fig. 5(a). The asymmetry in the Q^2 penalties between two sides of the central wavelength of the overlapping pumps is due to the uneven spectral shape of the pumps as shown in Fig. 3. In Fig. 5(b), a minimum guard-band of 2.8nm (2nm and 0.8nm for the blue- and red-shifted signal wavelengths respectively) around the central wavelength of the pump was required to ensure < 1 dB Q^2 penalty. A significant > 4 dB Q^2 penalty was also obtained on the signals remaining within 2nm of the 1508nm pump, whereas the Q^2 degradation was limited to only 1dB within the same vicinity of the 1485nm pump, mainly due to the 13dB lower level of RBS. We also observed negligible penalties on signals having a total wavelength separation of > 4 nm (considering both sides) from either of the overlapping pumps. Consequently, given the specific spectral profiles of the semiconductor laser diode pumps used in the experiment (Fig. 3), minimum 4nm guard-bands should be maintained around the pumps to obtain negligible penalties on the modulated signals from crosstalk and Kerr nonlinearities in the 150nm S+C+L band DRA under study.

We also calculated the Q^2 -factors from the derived SNR_{tot} in Eq. (1) and verified the model against the experimental results shown in Fig. 5. Here, $SNR_{ref}(\lambda)$ was obtained from the experimental data to give a reference result. It is clear from Eq. (1), when the RBS power is negligible, $SNR_{tot} = SNR_{ref}(\lambda)$ which means there is no penalty from the RBS, but all other transmission penalties are present. This is the case when a large enough spacing is maintained between the pump and signal. So, in the numerical model SNR_{ref} was calculated from the experimental curves of the Q^2 -factor as shown in Fig. 5, at points with no penalty from RBS and as close as possible to the pump wavelengths to minimise the impact of any unrelated wavelength dependent penalty on the Q^2 -factor, and considered here to be 17 dB and 20 dB with respect to the 1485 nm and 1508 nm pumps, respectively. The model provides very good estimation of the Q^2

penalties versus wavelength separation between the central wavelengths of the overlapping pump and signal. The inclusion of the pumps' spectral profiles ensures a good agreement between the model and experiment. It can be seen from the model that worst case Q^2 penalties at 1485nm and 1508nm are ~2dB and 15dB respectively, the higher penalties at 1508nm are mainly due to higher pump power and greater level of RBS induced crosstalk.

Additionally, using our numerical model for the dual-stage DRA considered here, we predicted the minimum guard-bands required to maintain 1dB Q^2 penalty at varying 3-dB linewidths of the overlapping Raman pump with a Gaussian spectral profile at 1508nm, as shown in Fig. 6. It is clear that Raman pumps with lower 3dB linewidth require smaller guard-band between the pump and signals, however there will be additional penalties from stimulated Brillouin scattering (SBS) due to such narrow linewidth pumps. Therefore, the linewidth of the overlapping Raman pump must be chosen carefully considering the trade-off between the penalties from SRS-induced crosstalk and SBS. According to the model prediction, more than 2.6nm guard-band should be kept around the central wavelength of the overlapping Raman pump (1508nm) with 3dB linewidth of 1nm in order to maintain < 1dB Q^2 penalty from SRS-induced crosstalk as shown in the insert of Fig. 6. This numerical prediction shows very good agreement with the experimental results obtained using the 1508nm semiconductor pump with ~1nm 3dB linewidth as shown in Fig. 5(b).

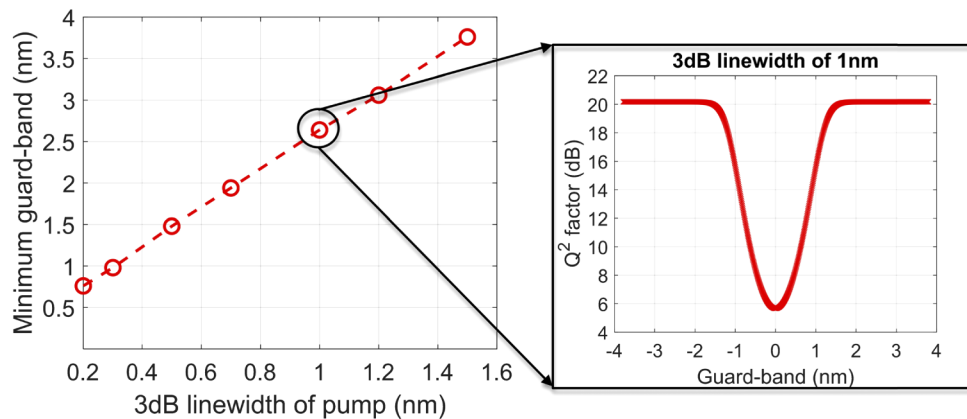


Fig. 6. Calculation of minimum guard-band requirement for 1 dB Q^2 penalty vs different 3 dB linewidth of the Raman pump at 1508 nm (Insert: Q^2 -factors vs required guard-band between the pump and signal for 1 nm 3 dB linewidth of the Raman pump).

5. Conclusion

We have experimentally and numerically investigated the transmission penalty from overlapping Raman pumps within the signal band of a practical UWB DRA with >13THz bandwidth. We have shown that the crosstalk penalty from the overlapping pumps depends mainly on the power level of the Rayleigh backscattering light of the pumps and is strongly influenced by the spectral shape of the pumps. The developed numerical model shows excellent agreement with the measured experimental Q^2 penalties. In a 150nm S+C+L band DRA with 15dB gain, an overlapping Raman pump having RBS level as large as the adjacent amplified signals, introduces more than 4dB Q^2 penalty on the 30GBaud PM-QPSK signals within 2nm of the pump. Additionally, a minimum guard-band of 4nm is required to ensure negligible transmission penalties from crosstalk. Based on the model developed and verified in this case, in UWB (>13THz) Raman amplifiers using commercial semiconductor laser diodes, guard-bands between the overlapping pumps and adjacent modulated signals must be designed carefully considering the trade-off between the overall effective amplification bandwidth and minimum crosstalk penalty.

Funding

Engineering and Physical Sciences Research Council (EP/M009092/1); H2020 Marie Skłodowska-Curie Actions (814276); Bundesministerium für Bildung und Forschung (16KIS0993).

Disclosures

The authors declare that there are no conflicts of interest related to this article.

Data Availability

The original data for this work is available at Aston Research Explorer (<https://doi.org/10.17036/researchdata.aston.ac.uk.00000466>).

References

1. A. Napoli, N. Calabretta, J. K. Fischer, N. Costa, S. Abrate, J. Pedro, V. Lopezk, V. Curri, D. Zibar, E. Pincemin, S. Grotz, G. Roelkensxi, C. Matrakidisxii, and W. Forysiak, "Perspectives of multi-band optical communication systems," in *OptoElectronics and Communications Conference (OECC)* (2018), paper 5B3-1.
2. J. K. Fischer, M. Cantono, V. Curri, R. Braun, N. Costa, J. Pedro, E. Pincemin, P. Doaré, C. Bouët, and A. Napoli, "Maximizing the capacity of installed optical fiber infrastructure via wideband transmission," in *International Conference on Transparent Optical Networks (ICTON)* (2018), paper Tu.B3.3.
3. F. Hamaoka, M. Nakamura, S. Okamoto, K. Minoguchi, T. Sasai, A. Matsushita, E. Yamazaki, and Y. Kisaka, "Ultra-wideband WDM transmission in S-, C-, and L-bands using signal power optimization scheme," *J. Lightwave Technol.* **37**(8), 1764–1771 (2019).
4. J. Renaudier, A. C. Meseguer, A. Ghazisaeidi, P. Tran, R. R. Muller, R. Brenot, A. Verdier, F. Blache, K. Mekhazni, B. Duval, and H. Debregeas, "First 100-nm continuous-band WDM transmission system with 115Tb/s transport over 100 km using novel ultra-wideband semiconductor optical amplifiers," in *43rd European Conference on Optical Communication (ECOC)* (2017), paper Th.PDP.A.3 (2017).
5. S. Namiki and Y. Emori, "Ultrabroad-band Raman amplifiers pumped and gain-equalized by wavelength-division-multiplexed high-power laser diodes," *IEEE J. Sel. Top. Quantum Electron.* **7**(1), 3–16 (2001).
6. M. A. Iqbal, P. Harper, and W. Forysiak, "Improved design of ultra-wideband discrete Raman amplifier with low noise and high gain," in *Advanced Photonics 2018 (BGPP, IPR, NP, NOMA, Sensors, Networks, SPPCom, SOF)*, *OSA Technical Digest* (online) (Optical Society of America, 2018), paper NpTh1H.2.
7. L. Krzczanowicz, M. A. Iqbal, I. Phillips, M. Tan, P. Skvortcov, P. Harper, and W. Forysiak, "Low transmission penalty dual-stage broadband discrete Raman amplifier," *Opt. Express* **26**(6), 7091–7097 (2018).
8. T. Tanaka, K. Torii, M. Yuki, H. Nakamoto, T. Naito, and I. Yokota, "200-nm bandwidth WDM transmission around 1.55 μm using distributed Raman amplifier," in *28th European Conference on Optical Communication (ECOC)* (2002), paper PD4.6.
9. A. H. Gnauck, R. M. Jopson, and P. J. Winzer, "Demonstration of counter-propagating Raman pump placed near signal-channel wavelengths," *IEEE Photonics Technol. Lett.* **29**(1), 154–157 (2017).
10. T. Naito, T. Tanaka, K. Torii, N. Shimojoh, H. Nakamoto, and M. Suyama, "A broadband distributed Raman amplifier for bandwidths beyond 100 nm," in *Optical Fiber Communications Conference* (Optical Society of America, 2002), paper TuR1.Top of Form.
11. T. Tanaka, H. Nakamoto, K. Torii, T. Naito, and I. Yokota, "Suppression of optical SNR degradation due to Rayleigh scattered pump light in broadband Raman amplifier," in *28th European Conference on Optical Communication (ECOC)* (2002), paper Tu.3.1.2.
12. M. A. Iqbal, L. Krzczanowicz, I. D. Philips, P. Harper, and W. Forysiak, "Noise performance improvement of broadband discrete Raman amplifiers using dual stage distributed pumping architecture," *J. Lightwave Technol.* **37**(14), 3665–3671 (2019).
13. M. A. Iqbal, L. Krzczanowicz, I. D. Philips, P. Harper, and W. Forysiak, "Evaluation of performance penalty from pump-signal overlap in S+C+L band discrete Raman amplifiers," in *Optical Fiber Communication Conference* (Optical Society of America, 2020), paper W4B.2.
14. C. R. S. Fludger, V. Handerek, and R. J. Mears, "Pump to signal RIN transfer in Raman fiber amplifiers," *J. Lightwave Technol.* **19**(8), 1140–1148 (2001).
15. M. A. Iqbal, M. Tan, and P. Harper, "On the mitigation of RIN transfer and transmission performance improvement in bidirectional distributed Raman amplifiers," *J. Lightwave Technol.* **36**(13), 2611–2618 (2018).
16. A. Richter, I. Koltchanov, E. Myslivets, A. Khilo, G. Shkred, and R. Freund, "Optimization of multi-pump Raman amplifiers," in *Optical Fiber Communication Conference and Exposition and The National Fiber Optic Engineers Conference, Technical Digest (CD)* (Optical Society of America, 2005), paper NTuB4.
17. G. C. Ferreira, S. P. Cani, M. J. Pontes, and M. E. Segatto, "Optimization of distributed Raman amplifiers using a hybrid genetic algorithm with geometric compensation technique," *IEEE Photonics J.* **3**(3), 390–399 (2011).

18. D. Zibar, A. M. Rosa Brusin, U. C. de Moura, F. Da Ros, V. Curri, and A. Carena, "Inverse System Design Using Machine Learning: The Raman Amplifier Case," *J. Lightwave Technol.* **38**(4), 736–753 (2020).
19. M. A. Iqbal, L. Krzczanowicz, P. Skvortcov, A. E. El-Taher, I. D. Phillips, W. Forysiak, J. D. Ania-Castañón, and P. Harper, "Performance characterization of high gain, high output power and low noise cascaded broadband discrete Raman amplifiers," in *19th International Conference on Transparent Optical Networks (ICTON)* (2017), paper We.D5.4.
20. M. A. Iqbal, M. A. Z. Al-Khateeb, L. Krzczanowicz, I. D. Phillips, P. Harper, and W. Forysiak, "Linear and Nonlinear Noise Characterisation of Dual Stage Broadband Discrete Raman Amplifiers," *J. Lightwave Technol.* **37**(14), 3679–3688 (2019).
21. M. A. Iqbal, M. Tan, L. Krzczanowicz, A. E. El-Taher, W. Forysiak, J. D. Ania-Castañón, and P. Harper, "Noise and transmission performance improvement of broadband distributed Raman amplifier using bidirectional Raman pumping with dual order co-pumps," *Opt. Express* **25**(22), 27533–27542 (2017).